Journal of Thermal Analysis, Vol. 47 (1996) 75-85

TIME-DOMAIN AND FREQUENCY-DOMAIN DIFFERENTIAL CALORIMETRY

C. Ferrari, G. Salvetti, E. Tognoni and E. Tombari

Istituto di Fisica Atomica e Molecolare – CNR, Via del Giardino 7, 56127 Pisa, Italy

Abstract

The heat capacity C_p of a sample can be considered as a frequency dependent quantity; its behaviour can reflect the dynamics of enthalpy fluctuations. In order to take into account the dynamic nature of the measured quantity, calorimetry can mimic experimental methods as those of dielectrometry, performing experiments in time domain or in frequency domain.

In this paper, an instrument is presented which is based on a calorimetric method meeting these requirements, and thus allowing to study sample dynamics of very viscous systems as glasses and some supercooled liquids. Moreover, experimental procedures permitting investigation of samples undergoing chemical and/or physical transformations by simultaneous measurements of enthalpy variation, heat capacity and, under certain conditions, thermal conductivity, are discussed.

Keywords: calorimetry, enthalpy, heat capacity, thermal conductivity

Introduction

The experimental apparatus and results reported here have been realized and obtained at the IFAM–CNR in Pisa during the last five years. At the beginning, calorimetry has been added to the experimental methods used in our laboratoires to study the liquid – solid phase transition of supercooled water.

To obtain very deep supercooling of a bulky liquid sample very thin capillary tubes [$\varphi_{in} \approx 0.5$ mm] were employed, which reduced the probability of heterogeneous nucleation. Commercially available calorimeters, particularly DSC systems, do not accept samples of this type, so it was necessary to design and construct a special microcalorimeter with fast response and high sensitivity [1]. Afterwards the instrument was successfully employed in studying biological solutions, phase-transitions, curing processes of thermosets, glass transitions, heats of solution of polymorphic materials, etc. [2]. Now we have at our disposal a variety of non-conventional calorimeters working in a wide temperature range and calorimetric cells for many different applications. The versatility of this technique comes from the possibility to use in the experiments the most suitable cell, a feature which is very important in enlarging the field of calorimetric applications.

0368–4466/96/ $ 5.00

John Wiley & Sons, Limited
Chichester

Why do we use the terms 'time-domain' and 'frequency-domain' calorimetry? These words are widely used in dielectrometry in which the response of a system to a small electric field is studied. The measured quantity, the dielectric constant, is frequency dependent and reflects the dynamics present in the sample. In a simplified picture, this means that the rotational diffusion of the electric dipoles in the sample shows a characteristic relaxation time τ, related to the intermolecular forces; in these conditions the dipoles can 'follow' the external field variations only at frequencies lower than $1/\tau$. The dielectric dispersion and absorption are resolved in a measurement if the experimental 'frequency window' is sufficiently large to cover the characteristic frequencies of the system.

Heat capacity is generally considered as a static thermodynamic quantity, in the sense that its values are time-averaged on the 'time window' of the experiment, which is usually much longer than the characteristic times of the 'internal modes'. But under certain conditions these modes can be made so slow that some of the characteristic relaxation times of the system become comparable with the experimental 'time window'. This may be the case of supercooled liquids and more generally of liquids near their glass transition temperature. This means that the sample temperature cannot 'follow' a power pulse applied to the sample. In this case, heat capacity and its measurement are frequency dependent like the dielectric constant [3].

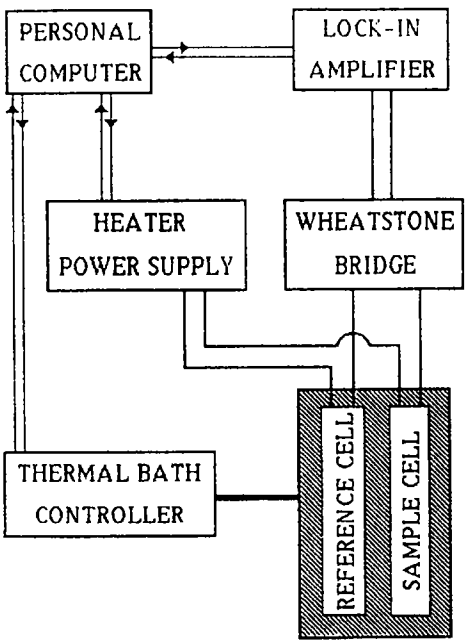

Fig. 1 Block diagram of the calorimeter

The analogy between dielectrometry and calorimetry extends also to the experimental procedures. Actually, with a 'power pulse' technique (time-domain calorimetry) or with an oscillating power signal at a frequency ω (frequency-domain calorimetry) [4] the complex heat capacity $C_p(\omega)$ can be obtained.

In this paper the main features and advantages of this kind of calorimetry developed at the IFAM, and its utilisation both for 'time-domain' and 'frequency-domain' experiments, will be discussed.

Time-domain calorimetry

In Fig. 1 is shown the schematic diagram of the calorimeter. It is essentially an isoperibol differential calorimeter equipped with a thermal bath controlled within ±0.01 K. Two twin cylindrical cells made of thin-walled stainless-steel tube, one for the sample, the other one for the reference substance, are assembled in thermally equivalent positions. The fundamental feature of the instrument is the temperature measuring probe: a thermoresistor uniformly wound on the cells to obtain the mean temperature of their lateral surface.

The temperature difference ΔT between the cells is related to the signals produced by the thermoresistors which are connected in the arms of a Wheatstone bridge working at a fixed frequency. The output of the bridge is measured with the sensitivity of a lock-in amplifier locked at the same frequency. Thus it is possible to measure ΔT values less than 10^{-5} K [5]. In this way noise and misleading signals arising from the presence of thermal gradients in the sample are strongly reduced.

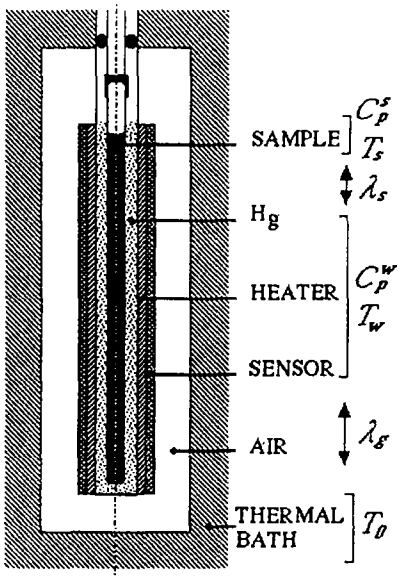

Fig. 2 A sketch of the longitudinal section of a calorimetric cell

The most important advantage of this technical solution is the possibility of an analytical description of the heat-transfer from the cell to the thermal bath. The cylindrical symmetry of the cell allows to make use of heat flow equations which are satisfactorily verified. Actually a very good fitting of the measured $\Delta T(t)$ profile can be obtained by changing the thermodynamic parameters of the sample in these equations. The fitting accuracy increases when the heat flow is essentially radial or the border effects are negligible (cell length >> cell diameter).

In Fig. 2 the longitudinal section of the cell is sketched. The heater wire, uniformly distributed near the sensor wire, supplies the input power signal which is needed for the absolute calibration and the measurement procedure [5]. The differential equations describing the sample calorimetric cells are:

$$C_p^s \frac{dT_s(t)}{dt} + \lambda_s[T_s(t) - T_w(t)] = 0$$

$$C_p^w \frac{dT_w(t)}{dt} + \lambda_g[T_w(t) - T_o] + \lambda_s[T_w(t) - T_s(t)] = P(t) + \frac{\delta \Delta H}{\delta t} \qquad (1)$$

where C_p and T are the constant pressure heat capacity and the temperature (s and w indicate the sample and the cell, respectively). λ_s and λ_g are the heat exchange coefficients between the sample and the cell, and between the cell and the thermal bath maintained at constant temperature T_o. $P(t)$ and ΔH are the power supplied to the heater and the enthalpy release due to the physical/chemical processes occurring in the sample, respectively [6]. When a power pulse $P(t)$, as that depicted in Fig. 3a, is supplied to the cell, the solution $T_w(t)$ of differential Eqs (1) is given as the sum of two exponential functions: the faster one describing the heat flow between the cell wall and the sample, the second one the heat flow between the cell and the thermal bath. In Fig. 3b the experimental curve, $T_{exp}(t)$, and the analytical solution, $T_w(t)$, are shown. The cell is thermodynamically characterised by the parameters C_p^w and λ_g; the sample by C_p^s and λ_s. The fitting procedure to determine the numerical values of $T_w(t)$ consists in changing C_p^s and λ_s until the theoretical curve overlaps the experimental one within the limits of the instrumental noise; the fitting accuracy $\delta(t) = T_{exp}(t) - T_w(t)$ is shown in Fig. 3c. The limiting sensitivities for C_p^s and λ_s measurements are $\pm 4.10^{-4}$ J K^{-1} and $\pm 4.10^{-3}$ W K^{-1}, respectively. The equivalent frequency of the experiment is $\omega_o = 1/\tau_o$ where τ_o is the observation time (Fig. 3a). The resulting C_p^s value takes into account only the 'internal modes' at frequencies higher than ω_o. In order to observe the contribution of slow dynamical modes to the heat capacity it is necessary to increase τ_o.

In our calorimetric cell it is generally verified that $\lambda_s >> \lambda_g$ and $C_p^s \leq C_p^w$, which means that it is possible to assume with a good approximation $T_w \cong T_s$. In this case, the solution of Eq. (1) reduces to a single exponential function describing the sample cell relaxation towards the thermal bath.

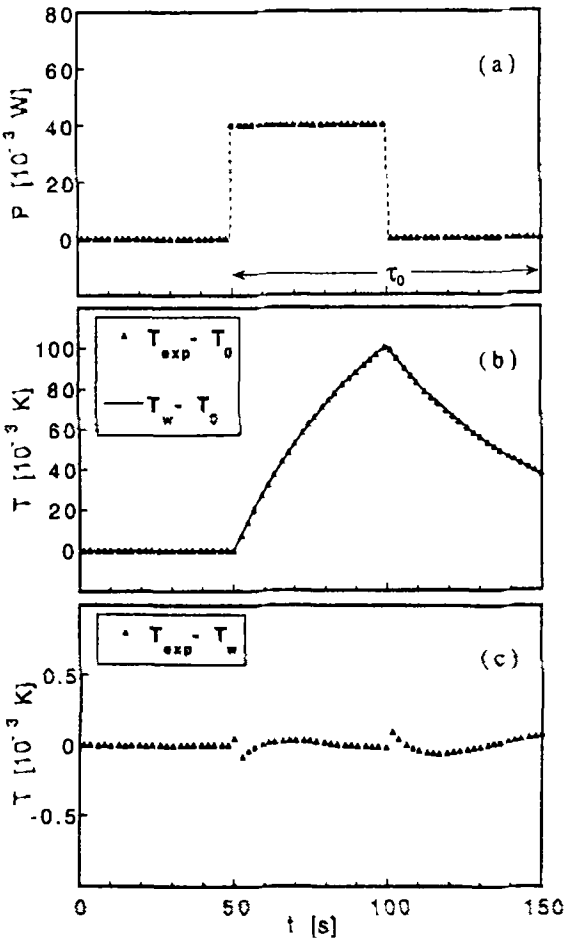

Fig. 3 The power pulse supplied to the cell is shown in (a); τ_0 is the experimental observation time. The measured temperature, $T_{exp}-T_0$ and the curve solution of Eq. (1), T_w-T_0, where T_0 is the bath temperature, are illustrated in (b). The fitting procedure to determine the numerical values of $T_w(t)$ consists in changing C_p^* and λ_s until T_w overlaps T_{exp} within the limits of the instrumental noise; the difference between the two curves is shown in (c)

A very interesting application of this method is represented by the simultaneous measurement of enthalpy variation and heat capacity of a thermosetting polymer during the curing process. Owing to the spontaneous rise in temperature induced by such reaction, until recently it has not been considered possible to measure C_p^* during the curing process.

Modulated DSC has been suggested only in the last two years as a method of measuring $\Delta H(t)$ and $C_p^*(t)$ simultaneously.

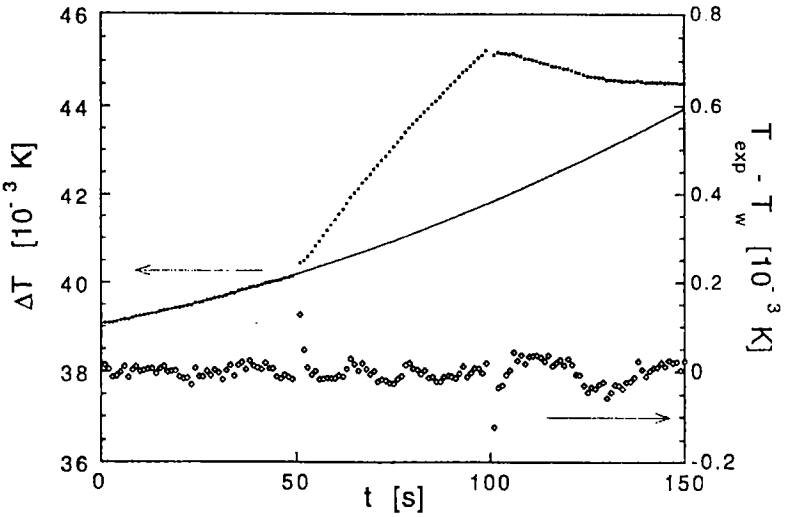

Fig. 4 Difference between sample cell and reference cell temperatures during the acquisition of one value of C_p^s. The open symbols represent the difference between the experimental points and the fitting values

The power pulse method and the differential calorimetry we have developed give a simple and reliable solution to this problem if $\Delta H(t)$ does not change appreciably during the observation time [6]. The computer-controlled procedure for C_p^s and ΔH measurements at fixed time intervals t_M is as follows:

i) the power pulse $P(t)$ (Fig. 3a) is supplied to the two cells;

ii) the temperature difference between the cells, $\Delta T(t)$, is recorded;

iii) the values of C_p^s and ΔH are calculated and stored on line by using a fitting procedure with the parameters defined through calibration.

If t_M is much greater than the cell thermal relaxation time towards the bath, $(C_p^s + C_p^w)/\lambda_g$, the temperature increase in the cells due to the power pulses practically reduces to zero when the subsequent run starts, and the $\Delta T(t)$ measured at that time is related to the rate of enthalpy release, $\delta\Delta H/\delta t$, by the equation

$$\frac{\delta\Delta H}{\delta t} = \lambda_g \Delta T \tag{2}$$

To calculate the heat capacity of the sample, it is necessary to subtract the effect of the enthalpy release on the measured $\Delta T(t)$. This effect is evaluated within the observation time, by extrapolating the profile of the $\Delta T(t)$ plot measured during the first 50 s preceding the power pulse (Fig. 4). The heat capacity of the sample can be calculated, with good approximation [6], using the following relationship:

$$\frac{\delta\Delta T(t)}{\delta t} = P[1/[C_p^w + C_p^s(t)] - 1/C_r] \quad (3)$$

From Eqs (2) and (3), where C_p^w, λ_g and the reference cell heat capacity, C_r are determined from calibration and ΔT and P are measured, it is possible to calculate both C_p^s and ΔH.

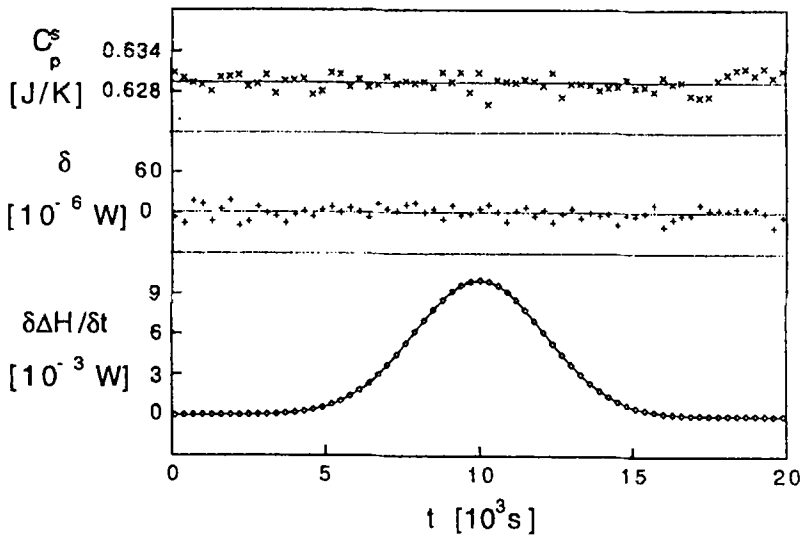

Fig. 5 Simulation experiment of the reliability test for the simultaneous measurements of C_p^s and $\delta\Delta H(t)/\delta t$. An additional input power $P(t)$, supplied to the sample cell to mimic an exothermic process with a Gaussian profile, is detected with an error of $\delta=[P(t)-\delta\Delta H(t)/\delta t]$ ($\bar{\delta}=0$, $\sigma=1.2\times10^{-3}$ J K^{-1}) while the C_p^s values are fitted to the heat capacity value of H_2O sample

The method and the calibration procedure possess high accuracy as it is shown by the reliability test in Fig. 5. The results in Fig. 6 refer to the curing of three samples of DGEBA-EDA thermosets at three different temperatures. The jump in the $C_p^s(t)$ curve marks the vitrification process and it represents the increasing 'difficulty' of the slow 'internal modes' to store the energy of the power pulse within the observation time τ_o. In other words, the measured heat capacity takes into account only the contributions of the 'internal modes' with frequencies higher then $1/\tau_o$.

Frequency-domain calorimetry

The frequency-dependent $C_p(\omega)$ values of liquids have been measured by various groups [3] who have deduced the structural relaxation time, the glass transition temperature and information on conformational changes of macro-

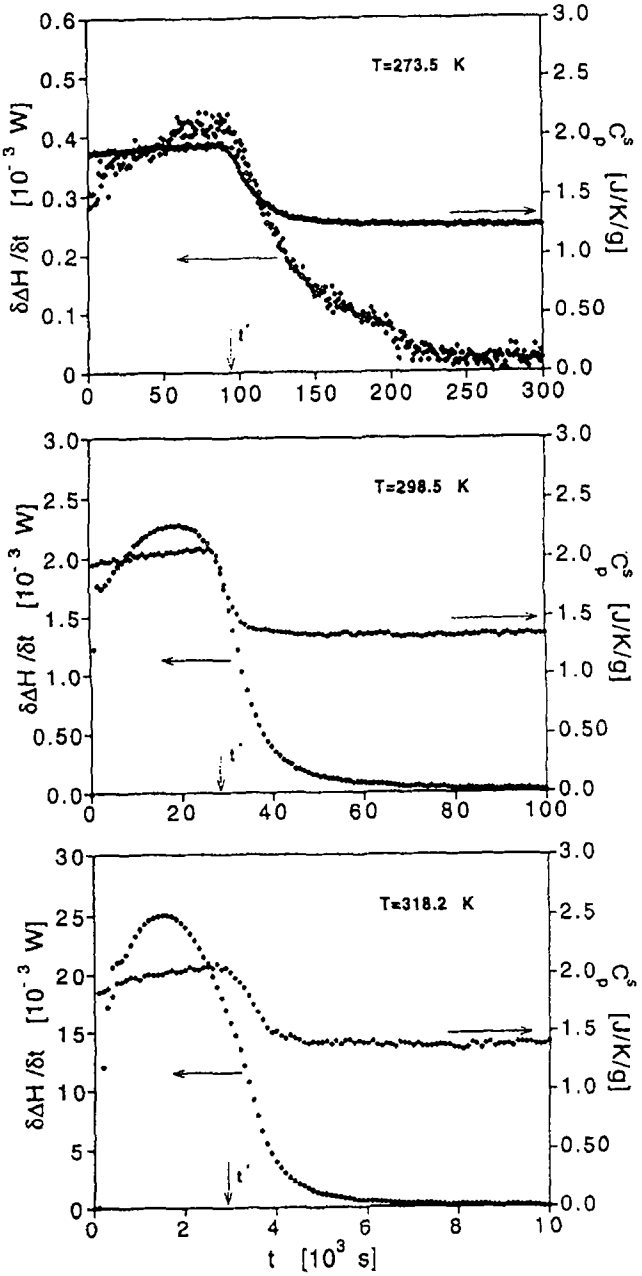

Fig. 6 Rate of enthalpy release and the simultaneous heat capacity data for three samples of DGEBA-EDA thermosets plotted against the reaction time at 273.5, 298.5, and 318.2 K, respectively. The vertical arrows mark the time of reaction at which the vitreous transition occurs

molecules in the sample. The experimental method introduced by Birge and Nagel (1985) [3] yields the product $C_p k$, where k is the thermal conductivity. To separate C_p and k it is necessary to perform two measurements with different geometry [7]. The technique we have developed removes the complication arising from the coupling of C_p and k and permits direct measurement of C_p even if the accessible frequency range is narrower. The experimental set-up is based on the differential calorimeter described above. The requirement for operating in the frequency domain is to excite the heaters of the two cells with an oscillating power $P(t)=P_o(1+\cos\omega t)$; discrete Fourier Transform is used to obtain the average value over one power signal cycle of the measured temperature $\Delta T(t)$ and the phase and amplitude of its component at the frequency of excitation ω, that is the complex quantity $T^*(\omega)$.

Within the linear response theory approximation, the calorimetric cell can be considered equivalent to an electrical circuit with distributed loss and storage components [8]. The change in amplitude and phase of the sample cell temperature, after an appropriate calibration procedure, can be converted into C_p' and C_p'', the real and the imaginary part of the complex $C_p^*=C_p'-iC_p''$. Under these experimental conditions T^* is related to C_p' by the relationship

$$T^* - T_o^* = A^* i\omega C_p^*/(1+ B^* i\omega C_p^*) \tag{4}$$

where T_o^* is the complex temperature response of the empty cell and A^*, B^* are temperature and frequency-dependent instrumental constants obtained by calibration with two reference samples. The accuracy of the method and the accessible frequency range depend on the geometry, the materials and the heat exchange coefficient of the cell. With a cylindrical cell (100 mm long, 5 mm external diameter) and the sample sealed in a Pyrex glass tube [$\varphi_{ex}=2$ mm, $\varphi_{in}=1.6$ mm] plunged in mercury, C_p^* can be measured within 1–2% at 10^{-2} Hz. From the numerical average of T^*over one power signal cycle the rate of the enthalpy release is simultaneously measured.

In Fig. 7 the results obtained with a sample of *n*-hexylamine (X) and diglycidyl ether of bisphenol A (Y) during the linear chain growth of the macromolecule (a structure of the type –X–Y–X–Y–) are illustrated.

C_p^* is real (the imaginary part C_p'' is negligible) and is coincident with the thermodynamic heat capacity until the number of the activated bonds in the sample or the mean length of the macromolecules is lower than a certain value. Under these conditions the dynamics of the 'internal modes' can follow the sample temperature variation; by increasing the macromolecule length, the dynamics of the modes related to the sample structure (the diffusion modes particularly) is so slow that the contribution of these modes to the heat capacity is practically lost; consequently the real part of the heat capacity decreases while the imaginary part goes through a maximum before returning to zero.

The enthalpy variation rate curve, simultaneously obtained, gives information on the number of covalent bonds created by the chemical reaction, i.e. on the structure, which affects dynamics.

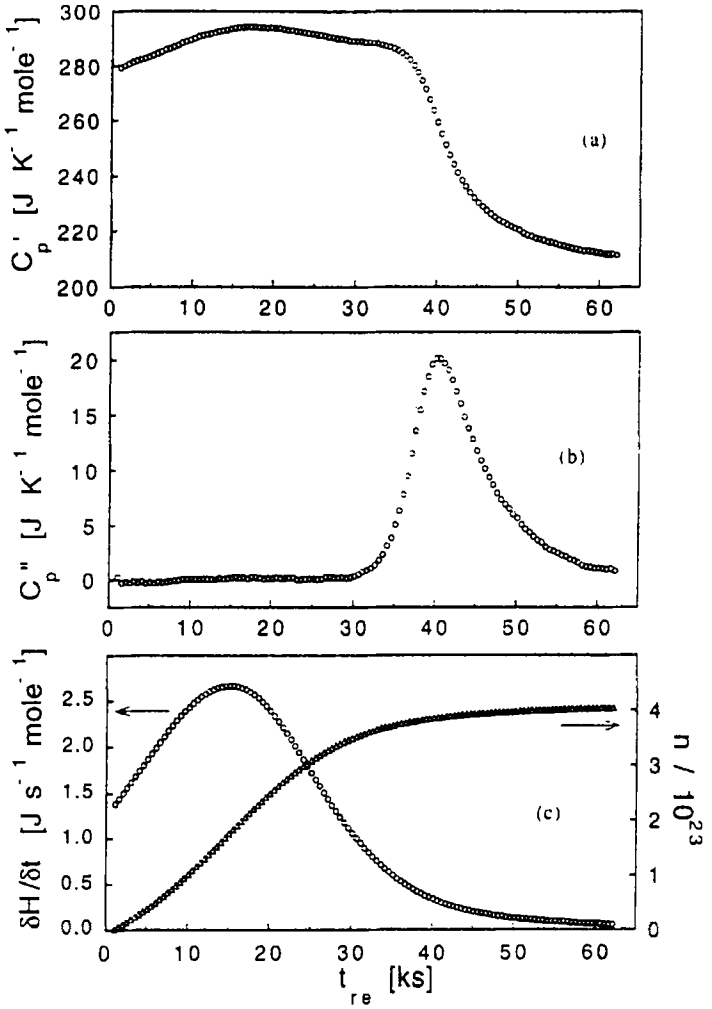

Fig. 7 The real (a) and imaginary (b) components of heat capacity at 0.01 Hz measured during the linear chain growth i.e., –X–Y–X–Y– structure, with X being *n*-hexylamine and Y, diglycidyl ether of bisphenol A at 300.1 K. In this process, the nitrogen atom of *n*-hexylamine covalently bonds with one terminal carbon atom of the epoxy groups of two Y molecules. (c) a plot *vs.* time of reaction of the heat release ($\delta H/\delta t$) and a plot of the number of covalent bonds formed as the reaction occurred

Conclusions

The main features of the calorimetric techniques developed in the last five years at the IFAM-CNR in Pisa, and two significant examples of their applications were reported. The aim has been to outline the potentiality of frequency-domain calorimetry to obtain information on the sample structure and dynamics.

Surely, in the future this new spectroscopic method will represent a powerful technique to be utilized jointly with dielectrometry, ultrasound spectroscopy and dynamic thermomechanical analysis in materials characterization.

References

1 D. Bertolini, M. Cassettari and G. Salvetti, Chem. Phys. Letters, 136 (1987) 67.
2 D. Bertolini, M. Cassettari, G. Salvetti, E. Tombari, S. Veronesi and G. Squadrito, Il Nuovo Cimento, 14-D (1992) 199; M. Cassettari, G. Salvetti, E. Tombari, S. Veronesi and G. P. Johari, Il Nuovo Cimento, 14-D (1992) 763; M. Cassettari, G. Salvetti, E. Tombari, S. Veronesi and G. P. Johari, J. Polym. Sci.: Polym. Physics: Part B, 31 (1993) 199; G. Salvetti, E. Tognoni, E. Tombari and G. P. Johari, in press on Thermochim. Acta (1996).
3 N. O. Birge and S. R. Nagel, Phys. Rev. Lett., 54 (1985) 2674; T. Christensen, J. de Physique, 46 (1985) 635; K. L. Ngai and R. W. Rendell, Phys. Rev. B, 41 (1990) 754; William W. van Osdol, Obdulio L. Mayorga and Ernesto Freire, Biophys. J., 59 (1991) 48.
4 M. Cassettari, G. Salvetti, E. Tombari, S. Veronesi and G. P. Johari, J. Non-Cryst. Solids, 172–174 (1994) 554; C. Ferrari, G. Salvetti, E. Tombari, G. P. Johari, Phys. Rev. Lett. (1995) submitted.
5 A. Barbini, D. Bertolini, M. Cassettari, F. Papucci, A. Salvetti, G. Salvetti and S. Veronesi, Rev. Sci. Instrum. 60 (1989) 1308; D. Bertolini, M. Cassettari, G. Salvetti, E. Tombari and S. Veronesi, Rev. Sci. Instrum., 61 (1990) 2416.
6 M. Cassettari, F. Papucci, G. Salvetti, E. Tombari, S. Veronesi and G. P. Johari, Rev. Sci. Instrum., 64 (1993) 1076.
7 P. K. Dixon and S. R. Nagel, Phys. Rev. Lett., 61 (1988) 341.
8 P. I. Somlo and J. D. Hunter, Microwave Impedance Measurements, IEEE Elect. Meas. Series 2, Short Run Press Ltd., Exeter 1985, p. 30.